Original Article

Radiologic–Histopathologic Correlation of Adult Spinal Tumors: A Retrospective Study

Abstract

Aim: Preoperatively performed magnetic resonance images (MRIs) are essential before treating spinal tumors surgically. This study aims to investigate the compatibility of MRI preliminary diagnosis and proven histopathologic diagnosis of consecutively operated 96 spinal tumors. **Material and Methods:** Medical records were retrospectively reviewed for all spinal tumors operated at our institute during a period of 6 years. One hundred and ten spinal tumors were detected. Fourteen tumors were excluded because they were not met our study criteria. **Results:** Ninety-six cases of spinal tumors were detected in 46 female and 50 male patients. The mean age was 49.3 ± 22.7 years. The most common symptom was radicular pain (88.6%). Histopathologic diagnoses were metastasis ($n = 26$), meningioma ($n = 16$), schwannoma ($n = 15$), ependymoma ($n = 9$), astrocytoma ($n = 6$), chronic nonspecific granulomatous infection ($n = 4$), lymphoma ($n = 3$), lipoma ($n = 3$), epidural tuberculosis abscess (Pott's disease) ($n = 3$), and other pathologies in 11 cases. Cervical spine was the less spinal region affected with metastases ($P < 0.05$). Thoracic spine was the most affected spinal region from meningioma ($P < 0.05$). Preoperatively, preliminary diagnosis on MRIs was proven with histopathologic examinations in 22 metastasis, 14 meningioma, 11 schwannoma, and all epidermoid cyst and lipoma cases. Despite the fact that MRI cannot diagnose all cases of spinal tumors, MRIs had a high accurate rate to diagnose the most common spinal neoplasms (69.8%). **Conclusions:** Metastases rarely occurred in cervical spine, whereas meningiomas were most likely to occur in thoracic spine. MRIs can help diagnose metastases and spinal benign lesions, whereas they failed to distinguish astrocytomas and lymphomas. Further prospective studies with large size are needed to support our results.

Keywords: *Ependymoma, histopathologic diagnosis, magnetic resonance imaging, meningioma, schwannoma, spinal metastases*

**Murad Asiltürk,
Anas Abdallah[1],
Erhan Özden
Sofuoglu**

Department of Neurosurgery, University of Health Sciences, Bakirköy Research and Training Hospital for Neurology Neurosurgery, and Psychiatry, [1]Department of Neurosurgery, Bezmialem Vakif University, Istanbul, Turkey

Introduction

Primary spinal tumors have infrequent incidence when compared with their cranial counterparts. Spinal tumors can be divided into two major groups: first one is primary tumors which originate from the spinal cord, meningeal, or bone cells. The second group is metastatic lesions which invade to spinal cord and surrounded tissues and take originate from other cells. Spinal tumors could present in nonspecific symptoms that require a significant suspicion for their diagnosis to be investigated.[1,2]

In 1887, after the description of spinal tumor resection by Sir Victor Horsley using laminectomy, the management of the spinal tumors had improved.[3] Despite that most primary spinal cord tumors are histopathologically similar to primary intracranial tumors, spinal cord tumors are 10 times less commonly seen.[1] As the clinical presentation could be nonspecific, the patients may present with serious radicular or local pain and motor dysfunction.[4,5] Therefore, most of the patients are wrongly diagnosed with degenerative spinal disease, cervical spondylopathy, or intervertebral disk herniation.[2,4,5]

Nowadays, magnetic resonance imaging (MRI) is considered as the gold standard for imaging of all neoplastic lesions. MRI provides accurate diagnoses and delineates the soft-tissue components.[4,5] Intraspinal tumors can cause serious deficits as well as the metastatic and

Address for correspondence:
*Dr. Anas Abdallah,
Department of Neurosurgery, Bezmialem Vakif University, Adnan Menderes Bulvari, Vatan Street, 34093 Fatih, Istanbul, Turkey.
E-mail: abdallahanas@hotmail.com*

high-grade malignant spinal lesions can be associated with high mortality.

Preliminary diagnosis using MRI can help to plan surgical intervention and to reduce complications that may occur from surgery. Preoperatively performed MRIs are essential before treating spinal tumors surgically. In this study, the authors aimed to investigate the compatibility of MRI preliminary diagnosis and proven histopathologic diagnosis of consecutively operated 96 spinal tumors. Furthermore, we investigated the relationship between involved spine region and tumor histopathologic diagnosis.

Material and Methods

Patient data, study design, and study criteria

Medical data and demographic characteristics were retrospectively reviewed for all spinal lesions which diagnosed and underwent surgery in our institute from 1992 to 1997. The patients who underwent only spinal operation for the spinal lesions were detected in MRI constituted the core sample for this study.

Inclusion criteria were: (1) the patients who underwent surgical resection (gross total resection [GTR], near-total resection [NTR], or subtotal resection [STR]) for spinal cord/column lesions (the patients underwent diagnostic biopsy were excluded); (2) a diagnosis of lesions was determined by MRI findings; (3) the patients had proven pathologic diagnosis upon the pathologic material obtained from spinal surgery; and (4) the age restriction was applied (only the patients older than 15 years were included).

Exclusion criteria were: (1) the patients who underwent resection for recurrent lesions; (2) a history of multiple malignant lesions in all organs of the whole body (patients known with multiple metastases); (3) the patients who underwent diagnostic biopsy; (4) presence of contraindication for performing MRI; and (5) the patients who underwent resection of the spinal lesion determined by computerized tomography (CT) only (if no preoperative MRI).

GTR was defined as resection whole tumor mass under a microscope; NTR was defined as removal more than 95% of tumor mass with leaving the tumor pieces attached to critical neural structure; if the resected tissue <95% and more than 75% of tumor mass, the surgical resection was defined as STR. These resections were seen under a microscope and confirmed with early postoperative MRI (in the first 24 h).[6]

This retrospective study was approved by the medical ethics committee of our hospital.

Evaluation of magnetic resonance images

Preoperative MRIs were performed according to the patients' symptoms. Each MRI was preoperatively evaluated by three independent senior radiologists using T1-weighted images (T1WIs) and T2-weighted images (T2WIs) with and without contrast-enhanced sequences obtained using contemporary MRI techniques. Each MRI was performed in three planes (sagittal, axial, and coronal). All three radiologists' evaluations were independently controlled by two senior neuroradiologists (one professor and one associated professor) who were blinded to the histopathological examinations of this study (radiologists and neuroradiologists did not participate in any part of operation or histopathological examination analysis, in the same way pathologists did not have any data about preoperative radiological diagnosis). The interobserver agreement was acceptable. Complete agreement was achieved in 82 of all 96 (85.4%) patients. A difference of one diagnosis between radiologists occurred in 11 (11.5%) assessments of the patients, a difference of more than a diagnosis for the same patient in 3 (3.1%) patients. The differences were solved by argument and the final evaluation was done after consensus among senior neuroradiologists about the last radiological diagnosis.

Statistical analysis

All data were expressed as the median or mean ± standard deviation with the range shown in parentheses. Univariate analyses were conducted to examine the association between radiologic and histopathologic features. Differences between groups were assessed by the Fisher's exact test and Student's *t*-test using the SPSS 21.0 statistical package SPSS 21.0 statistical package (IBM, Armonk, NY, USA). Significance was determined using $P < 0.05$, and trend-level effects were defined as $P = 0.05$–0.10. All P values were presented with an odds ratio (OR). OR was presented with 95% confidence interval (CI). When OR could not be calculated, risk ratio (RR) was calculated. All tests were two tailed.

Results

Patients' characteristics and surgical treatment

One hundred and ten spinal tumors were operated in our institute during the study. Fourteen tumors were excluded because they did not meet our study criteria. The remaining 96 spinal tumors were detected in 46 (47.9%) female and 50 (52.1%) male patients. The mean age was 49.3 ± 22.7 (16–87) years. The most common symptom was radicular pain (upper/lower extremity pain) (88.5%; $n = 85$), followed by motor deficit (87.5%; $n = 84$), loss of sensation (75.0%; $n = 72$), lower motor neuron findings including changing in reflexes (57.3%; $n = 55$), and sphincter dysfunctions such as urinary/fecal incontinence/retention (35.4%; $n = 34$). The mean duration of preoperative symptoms was 3.4 ± 7.8 (0.1–15) years. Metastases, high-grade glial tumors, and lymphomas had short preoperative course (short duration of symptoms) with an average of 2.6 ± 2.7 (1–5) months.

Meningiomas, schwannomas, and lipomas had relatively long preoperative course of 4.6 ± 6.9 (0.5–15) years on average [Table 1].

Thirty-two of 38 extramedullary located lesions underwent GTR/NTR (28 and 4, respectively), whereas 8 of 15 intramedullary located lesions underwent GTR/NTR (6 and 2, respectively). Thirty-four of 43 extradural lesions underwent GTR/NTR (18 vertebral, 10 epidural, and 6 vertebral + epidural). Intramedullary location was an independent factor to perform STR instead of GTR or NTR ($P = 0.032$; OR: 0.2 [0.06–0.82]).

Table 1: Baseline demographic and clinical characteristics of investigated 96 patients with spinal tumors

	Number of the patients (n=96), n (%)
Gender	
Female	46 (47.9)
Male	50 (52.1)
Age (years)	49.3±22.7 (16-87)
Location according dura	
Intradural	53 (55.2)
Extradural	43 (44.8)
Surgical resection	
Gross/near-total resection	74 (77.0)
Subtotal resection	22 (23.0)
Clinical presentation	
Radicular pain	85 (88.5)
Motor deficit	84 (87.5)
Loss of sensation	72 (75.0)
Lower motor neuron reflex	55 (57.3)
Sphincter dysfunction	34 (35.4)
Proven histopathological diagnosis	
Metastasis	26 (27.1)
Meningioma	16 (16.7)
Schwannoma	15 (15.7)
Ependymoma	9 (9.4)
Astrocytoma	6 (6.3)
Chronic nonspecific granulomatous	4 (4.2)
Non-Hodgkin lymphoma	3 (3.1)
Lipoma	3 (3.1)
Pott's disease	3 (3.1)
Epidermoid cyst	2 (2.1)
Hemangioblastoma	1 (1.0)
Ganglioglioma	1 (1.0)
Paraganglioma	1 (1.0)
CA	1 (1.0)
Osteochondroma	1 (1.0)
Germinoma seeding metastasis	1 (1.0)
Glioblastoma seeding metastasis	1 (1.0)
Disk material (no pathological tissue)	2 (2.1)
Preoperative course (years)	3.4±7.8 (0.1-15)

CA – Cavernous angioma

### Histopathologic diagnosis and locations of tumors

Histopathologic diagnosis was spinal metastasis in 26 cases [Figure 1], meningioma in 16 [Figure 2], schwannoma in 15 [Figure 3], ependymoma in 9 [Figure 4], astrocytoma in 6, chronic nonspecific granulomatous (CNSG) abscesses in 4, non-Hodgkin lymphoma (NHL) in 3 [Figure 5], lipoma in 3, epidural abscess (Pott's disease) in 3, and others in 11 cases (disk material in 2, epidermoid cyst in 2, hemangioblastoma in 1, osteochondroma in 1, ganglioglioma in 1, paraganglioma in 1, cavernous angioma in 1, cervical seeding metastasis of suprasellar germinoma in 1, and cervical seeding metastasis of glioblastoma multiforme in 1). In our metastasis patients, the most common primary tumors which caused metastasis to spine were tumors of the breast ($n = 7$) and prostate ($n = 7$), followed by tumors of the lung ($n = 5$), liver ($n = 2$), thyroid ($n = 2$), bone (metastasis of chondrosarcoma of humerus grade II) ($n = 1$), gastrointestinal ($n = 1$), and kidney ($n = 1$).

Locations according to dura: 53 cases were intradural lesions (38 extramedullary and 15 intramedullary) and 43 were extradural lesions (23 vertebral, 12 epidural, and 8 lesions were extended from vertebral body to epidural space). Locations of metastases were 14 in lumbar 9 in thoracic and 3 in cervical spine. According to these results, cervical spine was the less spinal region affected with metastases ($P = 0.041$; OR: 3.8 [1.02–13.8]). Locations for meningioma were 14 in thoracic and 2 in cervical. Thoracic spine was the most affected spinal region from meningioma ($P < 0.001$; OR: 0.1 [0.01–0.3]) [Table 2].

Accuracy of magnetic resonance imaging (compatibility of magnetic resonance imaging and histopathologic diagnoses)

Preoperatively, 26 tumors were preliminary diagnosed as spinal metastases on MRIs. Twenty-two of these 26 tumors were proven by histopathologic examinations to be spinal metastases (84.6%) ($P < 0.001$; OR: 0.06 [0.01–0.26]). The remaining four tumors were proven to be a meningioma, an NHL, and two of them to be CNSG infections (chronic abscesses). Preoperatively, 17 tumors were preliminary diagnosed as spinal meningiomas on MRIs. Fourteen of these 17 tumors were proven by histopathologic examinations to be spinal meningiomas (82.4%) ($P < 0.001$; OR: 0.023 [0.003–0.15]). The remaining three tumors were confirmed to be schwannoma in two cases and one else to be classic ependymoma WHO Grade II. Preoperatively, 15 tumors were preliminary diagnosed as spinal schwannomas (SSs) on MRIs. Eleven of these 15 tumors were proven by histopathologic examinations to be SSs (73.3%) ($P < 0.001$; OR: 0.05 [0.01–0.22]). The remaining four tumors were
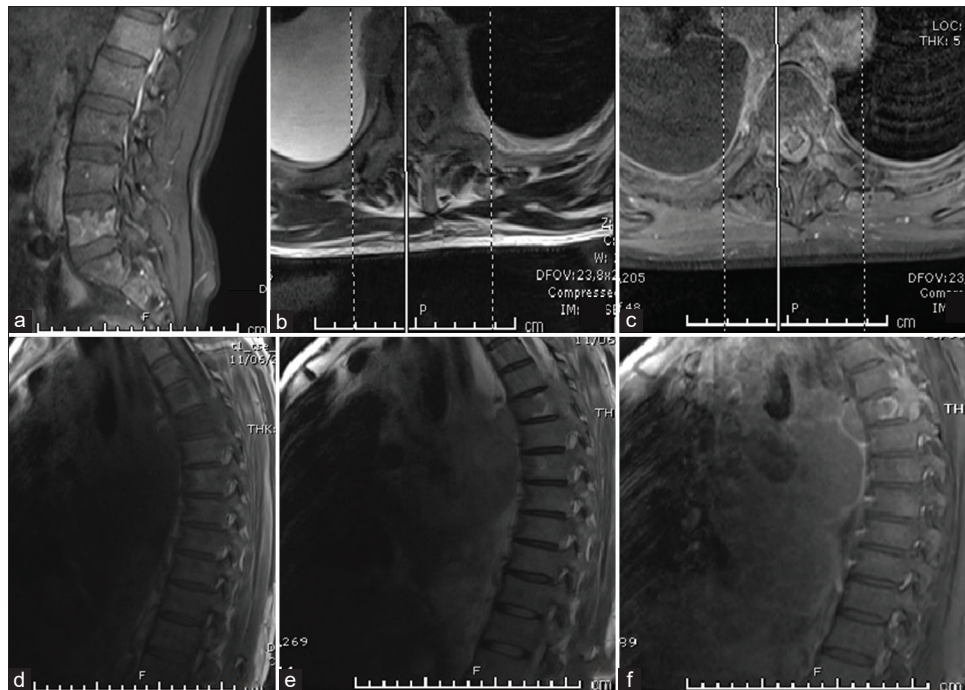
Figure 1: Lumbar and thoracic magnetic resonance images of a 54-year-old male patient who experienced dramatically developed paraparesis (last 1 week) and low back and both legs' pain for 1 month. The patient had a history of malign hepatocellular carcinoma for more than 2 years; (a) Sagittal contrast-enhanced T1-weighted image sequence of lumbar magnetic resonance imaging showed multiple involvements of L1, L2, L5, and S1 vertebral bodies. These vertebral bodies showed heterogeneous contrast enhancement. (b) Axial T2-weighted image of thoracic magnetic resonance imaging showed T5 vertebral body. (c) Axial T2-weighted image of thoracic magnetic resonance imaging showed T5 vertebral body was involved with heterogeneously contrast-enhanced hyperintense lesion extended to epidural space. Tumor mass surrounded the spinal cord like a muff. (d) Sagittal T1-weighted image sequence of thoracic magnetic resonance imaging showed multiple involvements of T4 and T5 vertebral bodies. Lesions were hypointense on T1-weighted image sequence. (e) Sagittal T2-weighted image sequence of thoracic magnetic resonance imaging depicts the "halo sign" with a hypointense metastatic lesion and a surrounding hyperintense rim in the T5 vetrebral body. (f) Sagittal contrast-enhanced T1-weighted image sequence of thoracic magnetic resonance imaging showed multiple involvements of T4 and T5 vertebral bodies. Note that rim be more apparent with contrast. He underwent the operation of STR and posterior instrumentation. The patient died on PO 5th month after involved with pneumonia
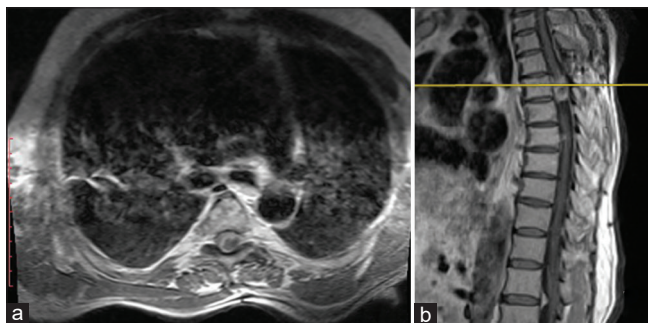
Figure 2: Lumbar and thoracic magnetic resonance images of a 66-year-old male patient who experienced back pain for 2 years. The patient had a history of T4 laminectomy before 20 years and biopsy for suspected prostate carcinoma, but the biopsy revealed no carcinoma cells. No history of neurofibromatosis type 2 was known; (a) Axial contrast-enhanced T1-weighted image sequence of thoracic magnetic resonance imaging showed a heterogeneously enhanced intradural extramedullary hypointense lesion at T5 level which was compressing the left side of the spinal cord; (b) sagittal contrast-enhanced T1-weighted image sequence of thoracic magnetic resonance imaging showed multiple involvement of intradural extramedullary lesion on T5, lesion at T7, and T12-L1 levels which was suspected to be metastasis. He underwent operation of near-total resection of intradural lesion at T5 level using laminectomy. The lesion was confirmed to be a meningothelial meningioma WHO Grade I. After physical therapy rehabilitation, the patient was doing well without recurrence
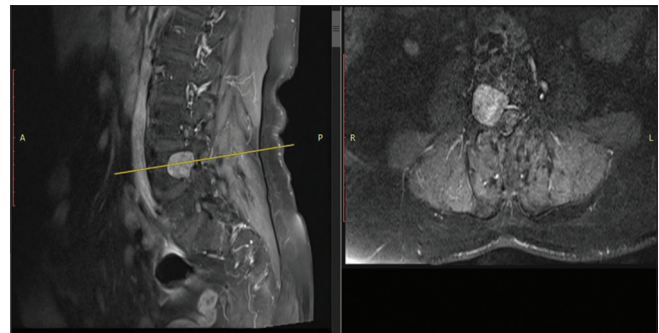
Figure 3: Lumbar magnetic resonance imaging of a 70-year-old female patient who experienced low back and right leg pain for 5 months. Contrast-enhanced T1-weighted image showed a well-circumscribed lesion which eroded right pedicle of L4 vertebra and measuring 27 mm × 28 mm × 16 mm, narrowed right L4 foramen, and showed heterogeneous enhancement after contrast substance on both of T1 and T2. She underwent operation and neurosurgeons distinguished that the lesion was intradural extramedullary intraoperatively. Gross-total resection had performed. The lesion was confirmed to be a schwannoma. The patient's pain relived and she was intact neurologically. On her postoperative 5th year control visit. Left side: Sagittal contrast-enhanced T1-weighted image; Right side: Axial contrast-enhanced T1-weighted image. Note the lesion showed moderate homogeneous enhancement, because of its location and eroded in the pedicle, and bony cancer was suggested, but schwannoma was considered in differential diagnosis

confirmed to be metastasis, meningioma, ependymoma, and disk material. Five out of 12 cases preliminary diagnosed as spinal ependymoma (SE) on MRI were confirmed to be ependymoma (41.7%) ($P = 0.02$; OR: 0.15 [0.03–0.71]).
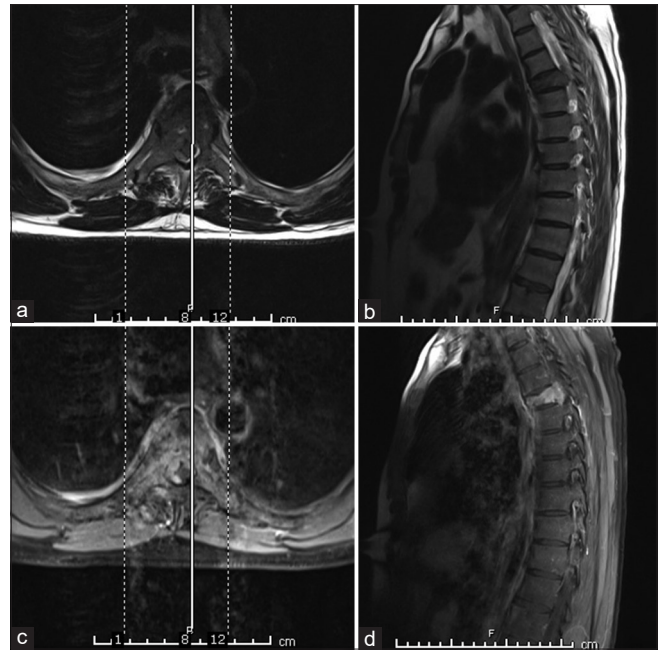
Figure 4: A 31-year-old male was referred to our emergency department with unsteady gait, left leg numbness, and weakness of 7 weeks. Retention of urine was developed in the last 3 days. Preoperative magnetic resonance imaging demonstrated the presence of well-circumscribed two intradural extramedullary lumbar lesions at L1-2 and S2 levels. The lesions were hyperintense on T1-weighted image and iso-hyperintense on T2-weighted image; (a) Axial T2-weighted image at S1 level; (b) Sagittal T2-weighted image. Gross total resection was performed for both lesions using T12 and S1 laminectomies and intraoperative neurophysiological monitoring. The lesion was confirmed to be a WHO Grade II classic ependymoma. The neurological examination did not change even the patient underwent 30 scenes of physical therapy and rehabilitation. No recurrence or seeding was detected on his 72th visit-control

Figure 5: Thoracic magnetic resonance images of a 49-year-old male patient who experienced dramatically developed paraparesis (last 10 days) and low back and both legs' pain for 3 months. The patient had a history of lesions in lungs and had undergone endoscopic biopsy before 2 weeks but the histopathologic examinations still unclear yet; (a) axial T2-weighted image sequence showed burst fracture of T4 corpus. The whole T4 vertebra was hypointense. (b) Sagittal T2-weighted image showed that T4 burst fracture compressed the spinal cord. (c) Axial contrast-enhanced T1-weighted image showed T4 vertebral body was collapsed and involved with heterogeneously contrast-enhanced hyperintense lesion extended to epidural space. (d) Sagittal contrast-enhanced T2-weighted image sequence. The lesion thought to be a lung metastasis. However, the lesion was confirmed to be a non-Hodgkin lymphoma lesion. He underwent operation of subtotal resection and posterior instrumentation

Compatibility of MRI and histopathologic examinations in our other cases and confirmed pathologic diagnoses are given in Table 3. Hypo-, iso-, and hyperintensity on T1WI, T2WI, and contrast-enhanced T1WI sequences of histopathologically confirmed and the most misdiagnosed four spinal pathologies are given in Table 4. Two of our six histopathologically proven WHO grade II astrocytomas showed no enhancement on contrast-enhanced T1WIs. There was no calcified spinal meningiomas. Despite the fact that MRI cannot diagnose all cases of these tumors, MRIs had a high accurate rate of up to 69.8% [Table 3].

Discussion

Spinal metastases can involve all tissues of spinal cord and column such as the bone, epidural space, leptomeninges, and medulla spinalis. The spinal region is the third most common site for metastatic neoplasms, following the lung and the liver,[7] as well as it is the most common osseous site.[8] More than two-thirds of systemic cancer patients experience spinal metastasis. Through a review of the literature, tumors of the breast (72%), prostate (84%), thyroid (50%), lung (31%), kidney (37%), and pancreas (33%) are the most common tumors with a high rate of metastasis to vertebrae and bones. All these tumors account for more than 80% of primary tumors in patients

presenting with spinal metastases.[9,10] Up to 95% of spinal neoplastic lesions are extradural lesions which can be divided into two major groups. The first group contained pure epidural tumors and the second one contained those taking origin from the vertebral bone and extending to the thecal sac through the epidural space.[11] The thoracic spine is most commonly involved with spinal metastases. In general, the prognosis for patients presenting with bone metastases is poor.[12] In our study, lumbar region was the most affected spinal region from spinal metastases. Maybe this related to our sample size which is relatively small.

Early published studies have shown that MRI can detect early bone marrow deposits as it has a significant impact on the evaluation of spinal neoplastic lesions.[13] MRI gives five specific relevant diagnostic information: the diagnosis of metastasis, the multiplicity of the lesions, the levels of involvement, the extent of the lesions, and the diagnosis of cord compression. The combination of unenhanced T1-weighted spin echo and short tau inversion recovery sequences has shown to distinguish benign from malignant bone marrow changes.[14] On T2WIs, due to their high water content, metastatic tumors are usually much brighter than normal bone marrow. Metastases often have a rim of

bright T2 signal around them (a halo sign). Diffuse signal hyperintensity and halo sign were shown to be strong indicators of metastatic lesions (sensitivity, 75%; specificity, 99.5%).[15,16] The bull's eye sign (focus of high signal intensity in the center of an osseous lesion) is a specific indicator of normal hematopoietic marrow (sensitivity, 95%; specificity, 99.5%).[15,16] Unfortunately, MRI cannot determine

all of spinal metastatic lesions. Distinguishing among changes related to treatment, traumatic acute fracture, and spinal tumors still a challenge for radiologists. In our study, 22 of 26 metastatic lesions were diagnosed using MRIs.

In our study, spinal meningiomas were the second most seen spinal lesions. The most of spinal meningiomas (90%) are intradural extramedullary lesions.[17,18] The remaining lesions either purely extradural tumors (5%) or have both intradural and extradural components taking on a dumbbell appearance (5%). Thoracic spine is the most affected spinal region from meningiomas;[18] this was in line with our results. Spinal meningiomas are almost located lateral to the spinal cord (60%–70%).[19] Cervical meningiomas are more likely to be located anteriorly compared to those in the thoracic spine.[15] Most meningiomas are solitary lesions (98%); however, multiple meningiomas are most often associated with neurofibromatosis type 2.[15] In a review through the literature, these lesions are usually isointense to slightly hypointense, possibly heterogeneous to medulla spinalis on T1WI sequences and isointense to slightly hyperintense to medulla spinalis on T2WI sequences and show moderate homogeneous enhancement on contrast-enhanced T1WI sequences. This is not always true for WHO grade II and III meningiomas.[15,17] There are some diagnostic features for typical meningioma that can facilitate the diagnosis of spinal meningiomas on MRI; they are well-circumscribed lesions which have broad-based dural attachment, dural tail sign (60%–70%), and ginkgo leaf sign in meningiomas arising lateral or ventrolateral to the medulla spinalis.[15,20] Occasionally, densely calcified spinal meningiomas are hypointense on T1WI and T2WI sequences, as well as calcified spinal meningiomas show only minimal contrast enhancement.[15,18] We did not have calcified spinal meningiomas in our series.

Table 2: Locations of investigated 96 patients with spinal tumors

Histopathological diagnosis	Cervical	Thoracic	Lumbar
Metastasis (*n*=26)	3	9	14
Meningioma (*n*=16)	2	14	-
Schwannoma (*n*=15)	5	4	6
Ependymoma (*n*=9)	4	1	4
Astrocytoma (*n*=6)	5*	1	-
Chronic nonspecific granulomatous (*n*=4)	-	-	4
Non-Hodgkin lymphoma (*n*=3)	1	2	-
Lipoma (*n*=3)	-	2	1
Pott's disease (*n*=3)	1	2	-
Epidermoid cyst (*n*=2)	-	1	1
Hemangioblastoma (*n*=1)	1	-	-
Ganglioglioma (*n*=1)	1	-	-
Paraganglioma (*n*=1)	-	-	1
CA (*n*=1)	-	1	-
Osteochondroma (*n*=1)	1	-	-
Germinoma seeding metastasis (*n*=1)	1	-	-
Glioblastoma seeding metastasis (*n*=1)	1	-	
Disk material (*n*=2)	-	-	2
Total	26	37	33

*3 astrocytoma were span from cervical region to thoracic but we accepted it as cervical because they largely occupied cervical more than thoracic spine. CA – Cavernous angioma

Table 3: Radiologic and histopathologic correlation in our series

MRI diagnosis	*n*	Confirmed	Misdiagnosed	Percentage	*P*	OR
Metastasis	26	22	CNSG abscess (2); Meningioma; NHL	84.6	<0.001	0.06 (0.01-0.26)
Meningioma	17	14	Schwannoma (2); Ependymoma	82.4	<0.001	0.02 (0.003-0.15)
Schwannoma	15	11	Metastasis; Meningioma; Ependymoma; Disk material	73.3	<0.001	0.05 (0.01-0.22)
Ependymoma	12	5	Metastasis; Schwannoma; Seeding GBM; Paraganglioma; Astro; CA; Disk	41.7	0.02	0.15 (0.03-0.71)
Astrocytoma	10	5	Ependymoma (2); Schwannoma; Seeding Germinoma; Ganglioglioma	50.0	0.58	0.3 (0.003-3.1)
Pott's abscess	5	2	CNSG abscess; Metastasis; NHL	40.0	0.032	0.04 (0.01-0.59)
NHL	3	1	Metastasis; Pott's abscess	33.3	0.2	0.1 (0.007-1.71)
Lipoma	3	3	-	100	<0.001	-
Epidermoid cyst	2	2	-	100	0.0014	-
CNSG abscess	1	1	-	100	0.1	-
Hemangioblastoma	1	1	-	100	0.067	-
Osteostoma	1	-	Osteochondroma	-	1.0	-
Total	96	67	29	69.8	-	-

MRI – Magnetic resonance imaging; CNSG abscess – Chronic nonspecific granulomatous abscess; CA – Cavernous angioma; NHL – Non-Hodgkin lymphoma; *P* – probability; OR – Odds ratio; *n* – Number of patients; Percentage – The accuracy percentage of MRI; GBM – Glioblastoma multiforme

The primary differential diagnosis of spinal meningioma consists of nerve sheath tumors (schwannomas) and ependymoma. SSs are typically located anteriorly compared to spinal meningiomas that are usually located posterolaterally. SSs have a tendency for multiplicity as they may have hypointensity central regions on contrast-enhanced T1WI sequences.[4,15] Several published studies suggested that typical SSs demonstrate iso- to hypointensity on T1WI, hyperintensity on T2WI, and postcontrast enhancement. Heterogeneous signal intensity and postcontrast enhancement are suggestive of internal hemorrhage and myxoid/cystic changes. There are additional imaging and pathologic features which suggest the diagnosis of SSs; however, they are not specific for SSs and also may be present in other neurogenic tumors including neurofibromas and malignant peripheral nerve sheath tumors. The most typical feature that may lead to diagnosing SSs is neural exits foraminal widening. This feature is more commonly seen with SSs than in spinal meningiomas.[4,15] A secondary sign that may suggest a neurogenic neoplasm is muscle atrophy within the affected nerve distribution.[4,15,18,21]

SEs are well-circumscribed neoplastic lesions. These puzzle lesions arise from ependymal cells lining the central canal, and they tend to occupy the central portion of the spinal cord and cause symmetric cord expansion; thus, they widened spinal cord.[5,22] Tumoral cysts associated with SEs are present in 22% and nontumoral cysts (cysts related to syrinx) are present in 62%.[22] Recently published several studies found that syringohydromyelia occurs in 9%–50% of SEs. This phenomenon is seen in cervical and intramedullary ependymomas more than other SEs.[4,22] In contrast to intracranial ependymomas, calcification is uncommon in SEs. Most SEs demonstrate iso- to hypointense on T1WIs; mixed-signal lesions are seen if cyst formation, tumor necrosis, or hemorrhage has occurred. However, most SEs are hyperintense on T2WIs. Occasionally, all SEs enhance postcontrast strongly somewhat heterogeneously on contrast-enhanced T1WI sequences. Peritumoral edema is seen in 60% of SEs. Association of SEs with hemorrhage leads to the "cap sign" (i.e., a hypointense hemosiderin rim on T2WIs) in 20%–33% of SEs.[15,22] The cap sign is suggestive feature but not pathognomonic

for SEs as it may also be seen in other spinal lesions such as hemangioblastomas and paragangliomas.[5,15,22] In our series, out of nine pathologically proven SEs, only five could diagnose correctly using MRI. Actually, on MRIs, 12 lesions thought to be SEs. In our study, SEs have a wide spectrum of images on MRIs and SE is not easy to be distinguished from other spinal lesions such as metastasis, schwannoma, astrocytoma, cavernous angioma, ganglioglioma, and seeding metastasis of intracranial tumors.

Spinal astrocytomas (SAs) usually span multiple segments in craniocaudal extent, with an average length of involvement of 4–7 vertebral body segments.[22,23] The most involvement spinal region from SAs is the thoracic spine followed by the cervical spine. SAs may involve both regions. SAs arise from cord parenchyma in contrast to SEs that arise in the central canal. SAs typically have an eccentric location within the medulla spinalis.[23] SAs may be exophytic and even appear largely extramedullary. These lesions usually have poorly defined margins (i.e., diffuse) which make its GTR is difficult. 40% of SAs have peritumoral edema on T2WI and FLAIR sequences. Despite the fact that the 20% of SAs have intratumoral cysts and 15% of SAs have peritumoral cysts, hemorrhage which is common in SEs is uncommonly seen. Although the SAs are varying in their WHO grades and showing various ranges of hypo- and hyperintensity, typical SAs show isointense to hypointense on T1WI sequences and hyperintense on T2WI sequences. The vast majority of SAs usually show patchy enhancement pattern on contrast-enhanced T1WI sequences. However, a few number of cases were reported to nonenhancing SAs.[23] In our study, two WHO Grade II astrocytomas showed no enhancement with contrast substances.

Intradural lipomas follow fat signal on all MRI sequences; that is meaning they are hyperintense on both T1WI and T2WI sequences, whereas they show no enhancement postcontrastly, as they are hypointense on fat-suppressed sequences.[15,24] One of the uncommon spinal lesions was spinal lymphoma (SL). SLs account for 3.3% of all central nervous system (CNS) lymphomas, which constitute only 1% of all lymphomas in the body.[25] The mean age at

MRI diagnosis	Sequences	Hypointense	Isointense	Hyperintense	Contrast
Astrocytoma	T1WI	2	4	-	4
	T2WI	1	1	4	
Ependymoma	T1WI	5	3	1	9
	T2WI	1	3	5	
Meningioma	T1WI	4	11	1	16
	T2WI	1	3	12	
Schwannoma	T1WI	4	10	1	15
	T2WI	1	3	11	

Table 4: Radiologic features of histopathologically confirmed and the most misdiagnosed four spinal lesions

T2WI – T2-weighted image; T1WI – T1-weighted images; MRI – Magnetic resonance imaging

Table 5: According to literature review, radiological features of the most common spinal lesions in our series

Tumor	T1WI	T2WI	C+T1WI	Characteristics
Metastasis	Varying?	Hypo- + halo sign	Hetero-	Heterogeneous enhancement. Diffuse signal hyperintensity and halo sign were shown to be strong indicators of metastasis[15,16]
Meningioma	Iso- to slightly hypo- possibly heterogeneous to spinal cord	Iso- to slightly hyper- to spinal cord	Moderate homo-	Moderate homo- enhancement; well-circumscribed lesions; broad-based dural attachment; dural tail sign (60%-70%); ginkgo leaf sign (especially for arising lateral or ventrolateral meningiomas)[20]
Schwannoma	Iso- (75%) to hypo- (25%)	Hyper (90%) (target sign)	Moderate homo-	Moderate homogeneous enhancement; sometimes heterogeneous with cyst; may be hemorrhagic or cystic lesions; randomly malign. These lsions sometimes show target sign (Hyperintense rim and hyperintense center) on T2WIs. Hypointense central regions on contrast-enhanced T1WIs. Foraminal widening at neural exits. Atrophic muscles within the affected nerve distribution[4,15,18]
Ependymoma	Iso- to hypo-; mixed signal if cyst+	Hyper- + peritu-moral edema	Somewhat hetero-	Somewhat hetero- strongly enhancement. SEs with hemorrhage leads to the "cap sign" (a hypo-intense hemosiderin rim on T2WIs) in one of 3 SEs[5,15,18]
Astrocytoma	Iso- hypo-	Hyper-	Usually patchy +	Patchy enhancement pattern;[15,22] Eccentric location within the spinal cord; May be exophytic, and even appear largely extramedullary; Have poorly defined margins; 40% of SAs have peritumoral edema on T2WI and FLAIR sequences[5]
Lymphoma	Iso-	Hyper- (?)	Solid Homo-	Solid homo- enhancement[15,25]
Lipoma	Hyper-	Hyper-	No	No enhancement[15]
Dermoid/epidermoid	Hyper-	Hyper-	No	No enhancement; may be presented with different malformations[15]

Iso- – Isointense; Hypo- – Hypointense; Hyper- – Hyperintense; SEs – Spinal ependymoma; SAs – Spinal astrocytomas; (?) – Uncommonly signal; T2WI – T2-weighted image; T1WI – T1-weighted images; MRI – Magnetic resonance imaging; FLAIR – Fluid-attenuated inversion recovery

presentation is 47 years. Females are more commonly affected. Patients involved with AIDS, transplant recipients, and congenital immunodeficient patients are the patients under high risk for developing CNS lymphomas. 85% of SLs are NHL.[15] The most common intramedullary location of SLs is the cervical region, followed by the thoracic spine.[15,25] Most SLs are solitary lesions; however, there may be multiple lesions throughout the spinal cord. Although spinal cord expansion is usually present, in some patients, there is relatively minimal enlargement of the cord. The lesions are generally poorly defined and tumoral cysts are generally not a feature and secondary syringomyelia is rare. Lymphoma usually does not have a hemorrhagic component. Reported SLs showed isointense to medulla spinalis on T1WI, hyperintense (uncommonly) on T2WI sequences, and they are usually solid and homogeneous enhancement. All three SLs were extended from vertebral corpus to epidural area.

Epidural abscesses are often seen in association with spondylodiscitis. Hematogenous dissemination from gastrointestinal, genitourinary, cutaneous, lung, and cardiac infection sources is also possible. Direct inoculation from iatrogenic procedures or trauma is an additional etiology of spinal epidural abscesses. The posterior epidural space is involved more often than the anterior epidural space. Peripheral enhancement with a necrotic core (abscess) or diffuse enhancement (phlegmon) may be seen on contrast-enhanced T1WIs. Fat saturation techniques make lesions in the epidural space more evident by suppressing the normal epidural fat.[1,15] In spondylodiscitis or osteomyelitis cases, T1WIs demonstrate endplate erosions with intradiscal fluid and patchy enhancement with contrast. The adjacent endplates demonstrate abnormal fluid marrow signal and enhancement. Osseous metastases typically do not cross the disk space from one vertebral corpus to the next. The absence of the vascularity in vertebral disks makes these disks are resistant to tumor invasion. This property can lead us to distinguish among both of the abscess and spinal neoplastic tumors.

In evaluating an MRI with an intramedullary enhancing lesion, the differential considerations include demyelinating disease, granulomatous process, cord infarction, cord vascular malformation, and primary cord tumor (such as astrocytoma, ependymoma, and hemangioblastoma). The differential diagnosis depends on several factors such as clinical presentation; previous medical history such as chronic diseases, alcohol abuse, or smoking; age; gender; CSF examinations; and evaluation of different MRI sequences. For an example, in demyelinating process the patient is usually a young female adult. Such patients can present with waxing and waning symptoms and the CSF examination findings showed a positivity for oligoclonal bands. Osseous metastases in a patient with a known primary malignancy would make an enhancing intramedullary lesion more suspicious for an intramedullary metastasis. Prominent vascular flow voids along the cord surface and intramedullary edema are

determining characteristics, indicating that a spinal lesion is an arteriovenous malformation.[1] Through a review of the literature and our experience, in Table 5, we summarized some important radiologic features of our most common spinal lesions on MRIs which can guide doctors to correct diagnosis.

The study has a few limitations: The used sample is composed of all documented spinal lesion cases which determined by MRI and histopathologically proven in our hospital over 6 years. The sample size is relatively small (*n* = 96). The sample does not represent a wide geographical area as all the patients are from our city and the surrounding area. The results represent a single-institute experience. Other institutes may have different results. The study design is retrospective. Further prospective studies with large size and long follow-up period are necessary to systematically investigate these findings.

Conclusions

MRI remains one of the most important diagnostic noninvasive techniques which should be performed before all surgical interventions for spinal lesions. Spinal metastases rarely occurred in cervical spine, whereas meningiomas were most likely to occur in thoracic spine. MRIs can help diagnose spinal metastases and spinal benign lesions, whereas MRIs failed to distinguish high-grade tumors such as astrocytomas and lymphomas. Further prospective studies with large size are needed to support our results.

Financial support and sponsorship

Nil.

Conflicts of interest

There are no conflicts of interest.

References

1. Chikani MC, Okwunodulu O, Mesi M, Mezue WC, Ohaegbulam SC, Ndubuisi CC. Surgically Treated Primary Spinal Cord Neoplasms in Southeastern Nigeria. J Neurosci Rural Pract 2018;9:137-9.
2. Emel E, Abdallah A, AF. Taking history and patient assessment in spinal surgery. In: Özer AF, Arslantas A, Dalbayrak S, editors. Principles of Spine Surgery. Vol. 1. Izmir: Intertip Inc.; 2017. p. 99-108.
3. Sellin JN, Tatsui CE, Rhines LD. Assessment and treatment of benign intradural extramedullary tumors. In: Winn HR, editors. Youmans and Winn Neurological Surgery. 7th ed. 2017. p. 2428-34.
4. Emel E, Abdallah A, Sofuoglu OE, Ofluoglu AE, Gunes M, Guler B, *et al*. Long-term surgical outcomes of spinal schwannomas: Retrospective analysis of 49 consecutive cases. Turk Neurosurg 2017;27:217-25.
5. Sofuoğlu ÖE, Abdallah A. Pediatric Spinal Ependymomas. Med Sci Monit 2018;24:7072-89.
6. Abdallah A, Emel E, Gündüz HB, Sofuoğlu ÖE, Asiltürk M, Abdallah B. Long-term surgical resection outcomes of pediatric myxopapillary ependymoma: Experience of two centers and brief literature review. World Neurosurg 2019. doi: 10.1016/j.wneu.2019.12.128.
7. Witham TF, Khavkin YA, Gallia GL, Wolinsky JP, Gokaslan ZL. Surgery insight: Current management of epidural spinal cord compression from metastatic spine disease. Nat Clin Pract Neurol 2006;2:87-94.
8. Klimo P Jr., Schmidt MH. Surgical management of spinal metastases. Oncologist 2004;9:188-96.
9. Alcalay M, Azais I, Brigeon B, Babin P, Vandermarcq P, Debiais F, *et al*. Strategy for identifying primary malignancies with inaugural bone metastases. Rev Rhum Engl Ed 1995;62:632-42.
10. Brage ME, Simon MA. Evaluation, prognosis, and medical treatment considerations of metastatic bone tumors. Orthopedics 1992;15:589-96.
11. Bartels RH, van der Linden YM, van der Graaf WT. Spinal extradural metastasis: Review of current treatment options. CA Cancer J Clin 2008;58:245-59.
12. Rosenthal DI. Radiologic diagnosis of bone metastases. Cancer 1997;80:1595-607.
13. Norman D, Mills CM, Brant-Zawadzki M, Yeates A, Crooks LE, Kaufman L. Magnetic resonance imaging of the spinal cord and canal: Potentials and limitations. AJR Am J Roentgenol 1983;141:1147-52.
14. Daffner RH, Lupetin AR, Dash N, Deeb ZL, Sefczek RJ, Schapiro RL. MRI in the detection of malignant infiltration of bone marrow. AJR Am J Roentgenol 1986;146:353-8.
15. Abul-Kasim K, Thurnher MM, McKeever P, Sundgren PC. Intradural spinal tumors: Current classification and MRI features. Neuroradiology 2008;50:301-14.
16. Schweitzer ME, Levine C, Mitchell DG, Gannon FH, Gomella LG. Bull's-eyes and halos: Useful MR discriminators of osseous metastases. Radiology 1993;188:249-52.
17. Setzer M, Vatter H, Marquardt G, Seifert V, Vrionis FD. Management of spinal meningiomas: Surgical results and a review of the literature. Neurosurg Focus 2007;23:E14.
18. Soderlund KA, Smith AB, Rushing EJ, Smirniotopolous JG. Radiologic-pathologic correlation of pediatric and adolescent spinal neoplasms: Part 2, Intradural extramedullary spinal neoplasms. AJR Am J Roentgenol 2012;198:44-51.
19. Schaller B. Spinal meningioma: Relationship between histological subtypes and surgical outcome? J Neurooncol 2005;75:157-61.
20. Yamaguchi S, Takeda M, Takahashi T, Yamahata H, Mitsuhara T, Niiro T, *et al*. Ginkgo leaf sign: A highly predictive imaging feature of spinal meningioma. J Neurosurg Spine 2015;23:642-6.
21. Murphey MD, Smith WS, Smith SE, Kransdorf MJ, Temple HT. From the archives of the AFIP. Imaging of musculoskeletal neurogenic tumors: Radiologic-pathologic correlation. Radiographics 1999;19:1253-80.
22. Smith AB, Soderlund KA, Rushing EJ, Smirniotopolous JG. Radiologic-pathologic correlation of pediatric and adolescent spinal neoplasms: Part 1, Intramedullary spinal neoplasms. AJR Am J Roentgenol 2012;198:34-43.
23. Seo HS, Kim JH, Lee DH, Lee YH, Suh SI, Kim SY, *et al*. Nonenhancing intramedullary astrocytomas and other MR imaging features: A retrospective study and systematic review. AJNR Am J Neuroradiol 2010;31:498-503.
24. Finn MA, Walker ML. Spinal lipomas: Clinical spectrum, embryology, and treatment. Neurosurg Focus 2007;23:E10.
25. Haque S, Law M, Abrey LE, Young RJ. Imaging of lymphoma of the central nervous system, spine, and orbit. Radiol Clin North Am 2008;46:339-61.